

Dynamics of hidden brain states when people solve verbal puzzles

Yuhua Yu¹, Yongtaek Oh², John Kounios², Mark Beeman¹

¹Northwestern University

²Drexel University

Author Note

This study was supported by NSF grant 1125596 to JK, and through the computational resources and staff contributions provided for the Quest high performance computing facility at Northwestern University which is jointly supported by the Office of the Provost, the Office for Research, and Northwestern University Information Technology.

Abstract

When people try to solve a problem, they go through distinct steps (encoding, ideation, evaluation, etc.) recurrently and spontaneously. To disentangle different cognitive processes that unfold throughout a trial, we applied an unsupervised machine learning method to electroencephalogram (EEG) data continuously recorded while 39 participants attempted 153 Compound Remote Associates problems (CRA). CRA problems are verbal puzzles that can be solved in either insight-leaning or analysis-leaning manner. We fitted a Hidden Markov Model to the time-frequency transformed EEG signals and decoded each trial as a time-resolved state sequence. The model characterizes hidden brain states with spectrally resolved power topography. Seven states were identified with distinct activation patterns in the theta (4-7Hz), alpha (8-9 Hz and 10-13 Hz), and gamma (25Hz – 50Hz) bands. Notably, a state featuring widespread activation only in alpha-band frequency emerged, from this data-driven approach, which exhibited dynamic characteristics associated with specific temporal stages and outcomes (whether solved with insight or analysis) of the trials. The state dynamics derived from the model overlap and extend previous literature on the cognitive function of alpha oscillation: the “*alpha-state*” probability peaks before stimulus onset and decreases before response. In trials solved with insight, relative to solved with analysis, the alpha-state is more likely to be visited and maintained during preparation and solving periods, and its probability declines more sharply immediately preceding a response. This novel paradigm provides a way to extract dynamic features that characterize problem-solving stages and potentially provide a novel window into the nature of the underlying cognitive processes.

Keywords: insight, creativity, problem-solving, hidden Markov model, EEG, dynamic modelling

1. Introduction

When people try to solve a problem, they often iterate through various stages spontaneously as they comprehend the problem, search the problem space, evaluate ideas, or discover the solution. These stages can be underpinned by discrete cognitive processes, perhaps subsuming distinct operations, cortical areas, or networks. Because the discrete processes can be difficult to discern within continuously recorded neuroimaging data, this poses a challenge for studying brain mechanisms of problem solving and other time-extended mental behaviors.

Furthermore, people can solve the same type of problems in different ways. Past research has found differential engagement of processes prior to solutions that participants report were achieved with sudden insight versus those achieved with more step-by-step analysis (Kounios & Beeman, 2014). Different paths to a solution may involve differentiable cognitive processes and brain areas or different weightings among these processes and areas. Additionally, these distinct solution paths may be characterized by the processes manifesting different dynamics: e.g., durations of processes, the transitions between them, etc. Such possibilities have not often been explicitly examined.

Neuroimaging with high temporal resolution provides a suitable tool to study the transient cognitive processes underlying problem-solving. Here we present a framework to segment observed data into a set of discrete and recurring *states* using a hidden Markov model (HMM). Each state is characterized by the scalp topography of electroencephalogram (EEG) spectral power, which reflects the sum of measurable neural processes ongoing at that moment. The model allows us to decode the data into a stochastic sequence of possible states on a trial-by-trial basis, across trials and participants. We investigate the dynamic characteristics of the states in relation to the different stages and outcomes of trials, i.e., whether and how people solved problems. The results can be compared to the existing literature on brain oscillatory activity underlying creative problem solving specifically, and human cognitive processes, generally.

1.1. Problems can be solved with insight or analysis

Creative problem solving involves a wide range of cognitive processes and neural substrates, and can vary in outcomes. People can solve problems in (at least) two general ways: with insight or with analysis. Insight is often characterized by a sudden reorganization of a mental representation of the problem (Sternberg, Davidson, & Simonton, 1995) while an analysis approaches the solution deliberately and incrementally, in a step-by-step manner (Webb, Little, & Cropper, 2016). Although these can somewhat overlap or both contribute to solving (especially for different steps in solving complex problems), insight and analysis reflect different search and evaluation strategies.

Previous work studying physiological correlates of insight have mostly used predefined signal construction: functional magnetic resonance imaging (fMRI) signal, EEG activity, or eye-tracking measures at a selected time range, time-locked to stimulus onset or to participant response, to study important processes engaged at specific moments of creative problem solving (Jung-Beeman et al., 2004; Kounios et al., 2006; Salvi et al., 2015; 2020).

While those studies have advanced our knowledge of brain mechanisms of insight, there are limitations. If the spatiotemporal scope of predefined signals is too narrow, the methodology risks missing significant markers. Conversely, defining the scope too liberally risks diluting the statistical power of the analysis.

A wholistic data-driven approach to EEG analysis can potentially uncover relevant signals from a wide range of spatial and frequency distribution. Because there are no behavioral

markers for problem solving stages other than an onset and a response, unsupervised machine learning techniques can be particularly suitable for this purpose. Unsupervised learning uncovers patterns in the data without prespecified labels. In this paper, we use an HMM, which is among the simplest and most-used methods in pattern recognition.

1.2. Hidden Markov models (HMM)

Hidden Markov models assume that a dynamic system is driven by a sequence of discrete states (see Rabiner & Juang, 1986, for the general theory) called a Markov chain. The states are mutually exclusive, recurring, and the probability of each state depends only on the prior state (i.e., state sequence is *Markovian*). Each state is associated with an *emission probability*, a distinct distribution of the observed data. Crucially, the state sequence is hidden and can only be inferred from the observables (Figure 1). A hidden Markov model is fully specified by an initial probability of a hidden state at the beginning, a transition probability matrix between states, and a set of emission probabilities. An expectation-maximization algorithm is commonly used to estimate the unknown parameters in a hidden Markov model. The sequence of hidden states can then be estimated by maximizing posterior probability based on the observables via a dynamic programming algorithm (see Methods).

In neuroscience applications, HMM provides a data-driven method to detect structures in high-dimensional data. It has been used to explore dynamic functional connectivity from magnetoencephalography (MEG) data under task and resting states (Baker et al., 2014; Quinn et al., 2018; Seedat et al., 2020; Vidaurre et al., 2018). In sleep studies, this data-driven method not only matches human experts in classifying sleep stages (Doroshenkov, Konyshev, & Selishchev, 2007), but also uncovered “a rich repertoire of brain dynamics underpinning the traditional PSG (polysomnography) stages” (Stevner et al., 2019)

HMMs have also been successfully applied to many Brain-Computer Interface (BCI) applications for differentiating task conditions (Williams, Daly, & Nasuto, 2018) or motor planning (Lederman & Tabrikian, 2012; Neuper et al., 2001). Finally, a potentially prolific paradigm has emerged to study population differences (e.g., with psychological diagnoses) using metrics derived from hidden states (Shappell et al., 2021).

Although there have been successes in using Hidden Markov type models in a range of applications, to our knowledge this approach has not been applied to decode a cognitive process like problem-solving in which component processes unfold spontaneously over time (with limited exception in animal work, Kemere et al., 2008).

HMM is both similar and dissimilar to other classification approaches. In HMM, the dynamics of the system are described by transitions between states in the state-time course. In contrast, methods such as ICA (Brookes et al., 2011) and micro-state analyses (Koenig et al., 2005; Lehmann & Skrandies, 1984) seek to decompose timeseries into sets of clusters without incorporating the temporal structure during model fitting. A comparison of these methods in the context of classifying EEG microstates can be found elsewhere (Rukat et al., 2016).

1.3. The current project

We adopt HMM as the generative model for a previously published EEG dataset (Erickson et al., 2018). EEG were recorded while participants attempted to solve compound remote associates (CRA), a verbal problem that can be solved with insight or analytically (Bowden & Jung-Beeman, 2003; Bowden & Jung-Beeman, 2007; Cranford & Moss, 2012). During each trial, a participant needs to read three problem words, search in his or her memory and come up with a word that can form compound words with each of the three problem words. Usually people solve about 33-67% of these puzzles within 15-20 seconds. Like many problems,

CRAAs can be solved via insight or via analysis. Given that previous work has shown that preparatory brain activity can bias people to either solve with insight or analytically, our epoch of interest included the time period from one second before onset until the moment of solution (or time-out, i.e., failure to solve).

The oscillatory patterns in the EEG signal provides a rich dimension to characterize cognitive processes. A vast amount of research has revealed that the brain communicates and implements cognitive functions utilizing different frequency bands, including frontal theta band (Cavanagh & Shackman, 2015), alpha band (Klimesch, Fellinger, & Freunberger, 2011; Klimesch, 2012), beta oscillation and gamma bursts (Lundqvist et al., 2016). Since insight problem-solving imposes multiple cognitive demands at the same time, we seek to represent the brain dynamics with the spatially resolved EEG power amplitude within those classic frequency bands. We focus on EEG power because, although there is considerable evidence that phase coupling (Grabner, Fink, & Neubauer, 2007; Rominger et al., 2020; Zhou et al., 2018) plays an important role in creative cognition, amplitude is the most widely used metric in insight related literature and therefore readily connects our results to prior work.

In this project, we attempt to fit the HMM to EEG time-frequency data to uncover distinct brain states. We then use the fitted model to perform trial-by-trial decoding and explore how each hidden state relates to different stages and outcomes of trials (whether solved with insight or with analysis). See Figure 2A for a schematic illustration. Due to the lack of studies using HMM for EEG frequency data in creative cognition, we did not predict specific frequency-spatial patterns that would be identified by the data-driven approach. It was therefore intriguing that the model extracted from the data a state featuring alpha-band activation. We were particularly interested in patterns involving the alpha frequency band because it has been widely studied in creativity and problem-solving literature. For example, higher alpha power is associated with generating more original ideas (Camarda et al., 2018; Fink et al., 2009); alpha power increases during the ideation stage and trends lower later in the trial (Schwab, et al., 2014); for review see Fink & Benedek, 2014). Furthermore, alpha-band activity at particular solving stages has been identified as one neural correlate of insight (Jung-Beeman et al., 2004; Rothmaler et al., 2017) .

2. Materials and methods

2.1. Participants

Experimental protocols were approved by the Drexel University Institutional Review Board. Fifty-one right-handed, native English-speakers gave informed written consent and participated in the study. Twelve of them were excluded for not following directions during the task (N=5), excessive EEG artifacts, (N=4) or not providing sufficient correct solutions (N=3). We analyzed the data from the remaining 39 subjects (see Erickson et al., 2018, for details).

2.2. Experiment Procedure

The detailed procedure was described in (Erickson et al., 2018). A graphical representation is shown in Fig. 2A. Briefly, each CRA puzzle was displayed on a monitor approximately 1.5m away from the seated subject. A fixation cross was displayed until participants initiated each trial by making a bimanual button-press with their thumbs on a computer mouse. At that time, crosshairs appeared around the fixation cross. After 1,000 ms, three CRA problem words (e.g., pine, crab, sauce) were displayed in a column replacing the fixation cross within the crosshairs. Participants were instructed to try to read all the words without moving their eyes and to think of a single solution word that forms a compound or familiar phrase with each of the problem words (in this case, apple, as in pineapple, crabapple,

applesauce). If they found an answer, they immediately indicate this by making another bimanual button press. Then “Solution?” appeared on the screen to signal participants that they should verbalize the solution after which the experimenter recorded whether the solution was correct. Participants indicated whether they had solved the problem by insight – that is, with the solution popping into awareness suddenly and seemingly disconnected from ongoing thoughts – or whether they had solved it analytically – that is, by working it out in a conscious, deliberate manner. Self-reports for insight or analytic solving processes have been widely used to study neural substrates underlying those strategies (e.g., Becker et al., 2020; Bowden, et al., 2005; Jung-Beeman, 2005; Jung-Beeman et al., 2004; Kounios et al., 2006; Laukkonen et al., 2018; Salvi et al., 2015; Salvi et al., 2020; Santarnecchi et al., 2019; Sprugnoli et al., 2017; Zhu et al., 2021). If a participant did not find a solution within 14 seconds, the computer displayed the fixation cross preceding the next trial. This procedure was used for 12 practice trials and 153 experimental trials. The stimuli were drawn from a normed database (Bowden & Jung-Beeman, 2003).

2.3. EEG Acquisition and Preprocessing

Eighty-four-channel EEGs were recorded (MANSCAN system, SAM Technology, Inc., San Francisco, CA) with tin electrodes embedded in an elastic cap (Electro-Cap International, Eaton, OH) using the extended International 10–20 System locations and digitally linked mastoids reference.

EEG preprocessing followed the procedure of Erickson et al. (2018) and was performed with Matlab 2015b (Mathworks, Inc., Natick, MA, USA) using the EEGLAB toolbox (Delorme & Makeig, 2004). The EEGs were downsampled to 250 Hz and high-pass filtered at 1 Hz. A series of semi-automatic artifact detection tools were applied to denoise the data: decreasing 60 Hz line noise (Cleanline plugin), bad-channel rejection and Artifact Subspace Reconstruction (Clean_rawdata plugin), interpolation for rejected segments and referencing to the global average. Continuous data were epoched to extract the time-period of interest: from 1,000 ms before onset to 500 ms after the button-press signaling a solution for solved trials, or a time-out marker. Trials that were solved within 2 seconds of stimulus onset were rejected since these are thought to be immediate recognition rather than problem-solving (Cranford & Moss, 2012), and would provide completely overlapping post-onset and pre-response period, invalidating the analyses related to trial stages. Independent Component Analysis was applied to further remove artifactual components (AMICA and MARA toolbox) on the epoched data. We imported the remaining data to SPM/EEG to perform a wavelet transformation and obtain the log-transformed power series at frequencies between 1 Hz and 50 Hz.

2.4. Hidden Markov Model (HMM)

We used a Gaussian HMM to model the EEG data in the time-frequency domain. Each hidden state is associated with a set of Gaussian distribution parameters (mean and covariance matrix) which prescribe the distribution of the features. The model parameters were estimated from the data (see Model Fitting). A flow chart for the processing and analysis steps is shown in Fig. 2B.

2.4.1. Feature processing

We constructed features by first downsampling the power series from the preprocessing step to 40 ms using a moving average. The nineteen channels of the International 10-20 System were used in the analyses below to reduce data dimensionality.

We bucketed the 1-50 Hz frequencies into 8 commonly used frequency bands (e.g., Kounios et al., 2008): Theta band (4-7 Hz), low and high Alpha bands (8-9 Hz and 10-13 Hz),

low and high Beta bands (14-17 Hz, 18-24 Hz), and three Gamma bands (25-29 Hz, 30-39 Hz, 40-50 Hz).

To normalize the power series, we computed the mean and standard deviation for each feature (per electrode and frequency band) per participant across trials. All the time series were then z -scored using each individual's means and standard deviations. We thus obtained a total of 152 normalized features (19 channels * 8 frequency bands).

2.4.2. Model fitting

Normalized timeseries from all epochs (including all trials and participants) were concatenated to calibrate the model using the expectation-maximization algorithm (Python package: `hmmlearn` 0.2.4). The parameters optimized by the algorithm are the initial probability of the hidden state at the beginning of an epoch, transition probabilities between states, and the means of the Gaussian distributions. We estimated the feature covariance matrix from all trials and used it as the covariance for the feature distribution in all the states.

The number of states is prespecified when fitting an HMM. A higher number of states is associated with higher model complexity and potentially more explanatory power at the cost of stability and interpretability. We aimed to strike a balance between those properties. We conducted analyses on the fitting results for the number of states ranging from 4 to 9. Because there is not yet a consensus on the best metric to compare the goodness of fit for HMM, we adopted two parametric measures: Bayesian Information Criterion (BIC) and Integrated Completed Likelihood (ICL) (Bertoletti, Friel, & Rastelli, 2015; Biernacki, Celeux, & Govaert, 2000). BIC has been widely used in model selection involving latent variables (Vrieze, 2012), whereas ICL can be seen as a modification on top of BIC that includes an additional entropy term to penalize the ambiguity of classification. Additionally, we computed an empirical likelihood measure with split-half cross-validation.

Besides the goodness of fit, the stability of the hidden states is also an important aspect. To evaluate the stability, we fitted the model from random split-half data using stratified sampling that maintained the same within-subject proportion of trial outcomes (solved with insight, solved with analysis, or unsolved). Eight iterations of split-half comparison were run for each state number. For each iteration, we calibrated model A and model B from the two halves of data. To measure how “different” the outputs of two model runs were, we computed the differences of the feature means from each pair of states (from two model runs respectively). We then averaged the differences across state pairs to obtain the overall “discrepancy”. Because the states were ordered arbitrarily from the fitting algorithm, the minimum discrepancy across all possible pairing schemes was used to index two model runs. Finally, the minimum discrepancies were average across 8 iterations. Lower discrepancy indicates higher stability of the model fitting.

2.4.3. Inference

The HMM extracts hidden state sequences from trial-by-trial decoding. Given the feature time series, the model estimates the posterior state probability at each time step. The hidden state with the highest probability is the most likely state. We analyzed the time-resolved probabilities of hidden states in relation to the stages of problem solving, in both stimulus-locked and response-locked manners. Given previous work, we are interested in examining the state dynamics pre-trial, throughout the attempt to solve, and for the last few seconds before response. We also examined the hidden-state dynamics in relation to how people performed on a given trial (not solved, solved with insight, solved with analysis).

The following metrics were used to summarize hidden-state statistics when people attempted the problems.

Average probability (occupancy). We computed the *average probability* of a state at a certain stage of a trial by averaging posterior probabilities across trials in a response-locked or stimulus-locked fashion. It is the average probability (across trials) at a certain instant, therefore we can also analyze its (temporal) rate of change and peak. When further averaging probabilities over a period, we obtained the state *occupancy*, i.e., the percentage of time spent in each state during that period.

Duration (sojourn time). The duration of a visit is the length time when the brain stays in a state without transitioning into a different one. The shorter the duration, the more transient a certain state is.

Visit frequency. The number of distinct visits to a certain state over a period is the visit frequency. The visit frequency does not consider the visit duration. Occupancy is closely related to the product of duration and visit frequency, therefore the three metrics are not independent. However, including all of them in the analyses and descriptions increases intuitive understanding of the model output.

We used two methods to align trials when computing the averages. One method used natural time, e.g., 1 second from the onset. With this method results are comparable to the traditional time-locked analysis. As an alternative approach, we aligned data with the number of transitions, e.g., the last N states before the response. Although the two approaches yield mostly similar results, they have complementary pros and cons when dealing with heterogeneity in state durations. Aligning with transitions provides novel perspectives accentuating the discreteness. For example, we can isolate the characteristic of the *last visit to a hidden state before response* without being affected by the varying durations of other states.

See Figure 2 for a flowchart for steps described above including the preprocessing pipeline, the feature construction, model fitting and inference, and a sample decoded trial as part of the model output. An additional, complete path of a sample trial that was solved with analysis is included in Supplement 2.

3. Results

3.1. Behavioral Results

Among 39 participants, an average of 127 ($sd=19$) trials were included in the analysis; of these, participants failed to solve 81 ($sd=21$) trials (time-out), solved 26 ($sd=14$) trials with insight, and solved 20 ($sd=11$) trials with analysis¹. Among all trials to which participants provided an answer, on average 6 ($sd=1$) incorrect responses were reported with insight, and 12 ($sd=2$) incorrect responses with analysis².

The average (and standard error) duration for trials solved with analysis was $6,720 \pm 102$ ms. The average duration for trials solved with insight was $5,680 \pm 94$ ms. The duration for a

¹ We included unsolved trials (time-outs) in the model fitting together with solved trials. Given we hypothesized that the same set of hidden states are involved in the course of problem-solving, it is reasonable to include time-outs in order to have sufficient data to calibrate the model.

² Given the small number of incorrect answers, especially those reported with insight, we did not include them in the analyses. Incorrect answers may be produced for various reasons and it is not appropriate to mix them together with correct answers in analyses for our purpose.

time-out trial was 14 s. Because trials solved with analysis were generally longer than those solved with insight, we also performed analyses sensitive to the response time on subsets of trials with equal RTs.

3.2. Model Fit

The two information criteria, ICL and BIC, both increase monotonically as the number of states increase (Figure 3, left-axis, red and blue lines). This indicates higher explanatory power and better fit (higher likelihood of observing the dataset) as model complexity increases, even after being penalized for additional degrees of freedom and entropy, consistent with other related work (Baker et al., 2014; Quinn et al., 2018). Out-of-sample likelihood from split-half cross-validation showed a similar pattern.

The stability analysis showed a non-monotone pattern (Figure 3, gray line and right-axis). Because the higher number of states is associated with greater number of parameters and the possibility of overfitting, discrepancy is expected to increase (or stability decreases) with the number of states. This was indeed observed for models with 6 states or higher. A low of number of states may also cause instability due to the nature of the discreteness. The discrepancy was the highest for the 5-state model. Visual inspection across iterations revealed that certain states were on the borderline of being identified at this level, and the competition between potential states created an all-or-none instability.

Major states identified by the models were robust with respect to the choice of state number. Visual inspection revealed a continuous evolvement of identified states as the number of states increased: certain states split into two new states, and certain states underwent a slight spatial rotation. See Supplement 1 for a comparison of $n=6$ and $n=7$.

For the rest of the paper, we present results from a 7-state model as it seemed to provide a good trade-off between stability and goodness of fit. Varying the number of states did not change our conclusions. (See Supplement 5 for additional results when using 6 and 8 states).

3.3. Hidden States

The estimated mean power values under each derived state are shown in Figure 4 as spatial heat maps for each frequency band. Distinct frequency-spatial activation patterns emerged for each state. State 1 was characterized by global activation in both lower and upper alpha-band frequencies. State 2 showed broad activation in the gamma band. State 3-7 showed different spatial distributions in theta-band activity with no significant activation or deactivation in the rest of the frequency bands. For convenience, we labeled those states as alpha, gamma, and theta 1 through theta 5, respectively.

As people attempted a problem, approximately equal time (occupancy) was spent in 6 out of the 7 states (Figure 5 left) and the least amount of time in gamma state. The duration of the states (Figure 5 right) mostly falls between [200 ~ 700] ms (25 ~ 75 percentile) during the solving period (between onset and response).

Interestingly, an “alpha-state” emerged from this data-driven approach. Since alpha power has been widely studied in creativity research (Fink & Benedek, 2014; Kounios & Beeman, 2014), results regarding the alpha-state can be reasonably compared to previous work. Therefore, rather than presenting an overwhelming number of results for each hidden state, we focus on the role of the alpha-state in the problem-solving process for the remaining of the Results section. For completeness we included the same analyses applied to the other six states in the Supplement.

3.4. Alpha-state and the stages of problem-solving

Alpha-state probability varies with the stages of problem-solving related to stimulus onset and response (Figure 6A). Regardless of the trial outcomes (solved or not), alpha-state probability peaked at onset, attenuated quickly as participants perceived and processed the stimulus. Furthermore, it trended downwards right before a response in solved trials.

Due to the temporal smoothing, it was not clear whether the alpha probability peaked before or after onset. Aligning trials by the number of state transitions (Figure 6B) indicated the peak occurred at 0 -- the last state before onset. In fact, comparing to all other states, the alpha-state was the dominant one, having the highest probability at the pre-onset moment (Table 1).

3.5. Alpha-state and different ways of solving a problem

As people worked on problems that they eventually solved with insight, they spent more time in the alpha-state compared to when they worked on problems solved with analysis (see Figure 6). To quantify the difference, we segmented a trial into four stages: pre-stage (1-second interval immediately before onset), onset stage (1-second interval immediately following onset), response stage (1-second interval before response) and solving stage (the trial period in between the onset and response stage). The corresponding z-score (insight – analysis) confirmed that alpha-state occupancy was significantly higher on insight trials than analysis trials during the pre ($z=2.35$), onset ($z=2.55$), and solving ($z=2.93$) stages (Figure 7). In addition to the occupancy, duration and visit frequency of alpha-state also exhibit a similar pattern of the “insight effect” during the first three stages.

Across the whole trial period, alpha-state visits were longer during trials when people solved with insight (582.6 ± 12.4 ms) than on trials when people solved with analysis (540.9 ± 13.7 ms; $z=2.27$, $p=0.02$). Recall that insight trials were on average *shorter* than analysis trials by about one second, it is therefore interesting to observe that insight trials were associated with *longer* visit to the alpha state. No significant differences in duration were found in other states (Figure 8).

3.5.1. Steeper decline of alpha-state probability is associated with solving by insight

As evident in the response-locked plot in Figure 6, the rate of decline of alpha-state probability was faster on trials solved with insight versus those solved with analysis: the decline started later and was steeper prior to people solving with insight than solving with analysis. For example, the probability changed during the last 1.5 s before the response was -0.12 ± 0.01 for insight trials, lower than -0.07 ± 0.01 for analysis trials ($z=-3.57$, $p<0.001$). The significant difference between the two rates of change was robust and did not depend on the specific sampling points (Fig. 9). Even though trials solved by insight were on average shorter than those solved by analysis, the difference in RT cannot account for the different rate of change in probability (See Supplement 6 for the same analysis performed on a subset of trials where the two types of the trials have similar RT distribution).

In other words, participants responded sooner after transitioning away from the alpha-state when ultimately reporting insight. Using trial-by-trial state sequences, the last alpha-state was on average 1.13 transitions closer to response on insight trials versus analysis trials [$z=3.77$, $p<0.001$] (Table 2). The duration of the last alpha-state was 87 ms longer than those on analysis trials [$z=3.22$, $p=0.001$].

4. Discussion

People spontaneously engage various cognitive processes when attempting to solve a problem. Problem-solving stages are likely distinct (considering processing the prompt versus evaluating a solution) but difficult to disentangle from continuously recorded neuroimaging data.

We present a paradigm to segment EEG data, recorded while participants attempted to solve problems, into discrete states using a hidden Markov model. This data-driven approach uncovered a set of brain states characterized by spatial-frequency activation maps. Importantly, the dynamic characteristics of the states are associated with different stages and outcomes of trials. As discussed in detail below, the results overlap with and extend prior literature.

A seven-state HMM provided stable fit to the data that balanced between explanation power and interpretability. One of the states exhibits widely distributed alpha-band activity; one state features gamma-band activity; and the remaining five feature theta-band activity with distinct spatial distributions.

We focused on the alpha-state dynamics in this paper because alpha-band oscillation has been widely studied in human creativity, and therefore a rich literature exists. The alpha-state dynamics varied by the overall temporal stages of a trial (from onset to response), as well as by the manner of reaching a solution.

Participants are most likely to occupy the alpha-state right before the stimulus appears and quickly transition away from it as they perceive and process the stimulus. Furthermore, the average alpha-state probability attenuates and quickly declines before participants solve the problems. The peak alpha-state probability at onset is analogous to event-related alpha power synchronization (ERS), while the decrease in probability, both after onset and before response, corresponds to an event-related desynchronization (ERD). Similar ERS and ERD patterns around onset and response have been robustly demonstrated in tasks posing moderate cognitive demand (Cao, Li, Hitchman, Qiu, & Zhang, 2015; Freunberger, Klimesch, Griesmayr, Sauseng, & Gruber, 2008; W. Klimesch, Doppelmayr, Pachinger, & Russegger, 1997; W Klimesch, Doppelmayr, Schwaiger, Auinger, & Winkler, 1999). ERS putatively reflects the suppression of irrelevant information; while ERD reflects the recognition and retrieval of semantic information (W. Klimesch et al., 2011). These interpretations fit well with our observations.

The second set of results shows that alpha-state dynamics differ on trials that were subsequently reported to be solved with insight versus solved with analysis. Immediately before solving with insight, compared to solving with analysis, participants linger in alpha-state longer and initiate the button-press sooner once transitioning away from the alpha-state. This *insight effect* corroborates with and extends previous results. Jung-Beeman et al. (2004) reported that in the final moments prior to solution alpha power (estimated at 9.8 Hz) over right posterior parietal cortex is higher on trials solved by insight than trials solved with analysis. The sharper decline in alpha-state probability observed in the current study immediately preceding response may be associated with the subjective feeling of suddenness that accompanies an insight. ERD is often seen as an electrophysiological correlate of excitatory process. For example, the magnitude of ERD is correlated with how semantically integrated the retrieved information is (Klimesch, 2012). It is therefore reasonable to speculate that an insight solution, known for its wholistic nature (Schooler & Melcher, 1995), elicits more cortical excitation (Salvi et al., 2020) and therefore a steeper decline in alpha-state probability, relative to a solution achieved by step-by-step analysis.

The interaction between the alpha-state and the manner of problem-solving is not limited to the pre-response period. When people eventually solve with insight, they are more likely to occupy the alpha-state during the one-second preparation period prior to problem presentation, as well as during the solving period. It is not surprising to see this alpha-state bias, given that alpha power is positively associated with high creative performance (Camarda et al., 2018; Fink et al., 2009; Grabner et al., 2007; Martindale & Mines, 1975; Schwab et al., 2014). The insight effect

during the preparatory period suggests that participants can be in a brain state relatively conducive to solving with insight, even before knowing what the problem is. Prestimulus brain activity examined with fMRI and EEG has been shown to bias people to solve puzzles in an insight-leaning versus analysis-leaning manner (Kounios et al., 2006; Subramaniam, Kounios, Parrish, & Jung-Beeman, 2008; Zhu et al., 2021). The observed pre-stimulus insight effect might be related to the processing bias modulated by the alpha oscillation. There is evidence that alpha power in many cortical areas is inversely related to measures of cortical excitability (Chapeton et al., 2019). In perceptual decision tasks, lower prestimulus alpha power leads to higher hit and false alarm rates (Samaha et al., 2020). It is possible that, in the context of solving a CRA, low alpha-state probability before onset biases cognitive process towards a more active approach, evaluating salient solution candidates for prompt words one by one, which would be reported as “solving with analysis.” (Kounios et al., 2006).

While results here are comparable to the alpha effects in earlier studies of creative cognition, they also provide novel perspectives from the bottom-up approach. It’s important to note that the states in the current paradigm were derived differently from, say, measures of alpha power at a particular electrode (or region) at a particular time (e.g., Fink et al., 2009; Jung-Beeman et al., 2004). Hidden states are identified by classifying the spectral power distribution in the temporal and spatial dimensions simultaneously. The alpha-state emerges from this data-driven approach as one featuring distributed alpha-band activity, and it was typically returned to several times throughout the period as people attempted to solve problems. Compared with traditional methods that rely on predefined signals, the data driven approach may capture previously neglected patterns without overly undermining statistical power due to multiple comparison. Furthermore, trial-by-trial path modelling allows us to draw inferences on the dynamic characteristics, such as the visit duration and transition patterns, of the underlying cognitive process. This yields novel findings that are not directly amenable to traditional methods.

Exploratory analyses suggest that the gamma state and some theta states also show distinct dynamics related to the temporal stages as well as the outcome of a trial (Supplement 3 and 4) although not as robust as the alpha-state. Therefore, to avoid overinterpretation and false discoveries, we leave those results as potential hypotheses for future projects.

One of the limitations of the current project comes from data constraints. The current dataset, including 39 subjects and more than 100 trials for each, is adequate for testing pre-defined hypothesis or certain exploratory analyses. But like any other machine learning approach, the power weakens as we expand the hypothesis space. As a result, we settled on a seven-state model fit, even though some evidence suggested that seven is not the upper limit for the model’s explanatory power. The current approach identified a single alpha state with wide spread activation, therefore we cannot characterize the spatial distribution in the context of creative cognition as reported in prior work (Di Bernardi Luft, Zioga, Thompson, Banissy, & Bhattacharya, 2018). With more data, a similar model should be able to extract more granular characteristics from a higher-dimensional (with a larger number of states) structure. In particular, some states in the current model may subdivide into multiple stable substates. The global alpha-state splits (from the current 7-state model) into 2 spatially distinct states in an 8-state HMM. Although the collective dynamics of these two states are consistent with the results presented in this paper (Supplement 5), there is evidence for their differentiable involvement in the problem-solving process. Furthermore, we have adopted a group-average approach in essence, as data from all subjects, after normalization, were concatenated to fit a single model. Individual

differences in both problem-solving (and cognition generally) and EEG spectrum patterns are well-known. An experiment paradigm like precision functional mapping (Gordon et al., 2017) that collects hours of data from a single subject might enable better spatially-resolved state analyses.

Limited by the current computational capacity, we chose to model a subset (19 channels) out of the original 84 channel recording. With the current setup each model fitting takes 20 – 30 hours on a High-Performance Computing cluster. Increasing the data dimension 4 folds would render the process unwieldy. Future work would benefit from dimension reduction methods, such as Independent Component Analysis (Makeig et al. 2004; Onton et al., 2006) to utilize the full dataset. Spatial resolution is always a challenging issue in EEG studies (Nunez et al., 1994; Tenke & Kayser, 2012). The group-average approach in the current model fitting further reduce the resolution due to individual anatomical differences. However, many techniques have been developed to align group data and to extract spatial information from EEG data (Calhoun et al., 2009; Janssen et al., 2020). Future work can incorporate those methods in feature construction to increase the spatial granularity of HMM results.

The current project explored the temporal structure in the power amplitude topographies. There is considerable evidence that phase coupling (Grabner et al., 2007; Rominger et al., 2020; Zhou et al., 2018) plays an important role in creative task performance. Vidaurre and colleagues (2018) reported that phase coupling, while providing unique information, made a smaller contribution in driving HMM segmentation compared to the power signals. Some authors (Quinn et al., 2018; Vidaurre et al., 2018) have developed novel HMM paradigm that captures power and coupling features simultaneously. Future projects would benefit from including phase information in the modelling framework along with amplitude.

The current project develops a novel paradigm to study dynamic, multi-component cognitive processes. Here, this data-driven approach yielded results that corroborated and extended previous literature on creative problem solving. Furthermore, this approach provides a powerful tool to derive hypotheses for future studies.

References

- Baker, A. P., Brookes, M. J., Rezek, I. A., Smith, S. M., Behrens, T., Smith, P. J. P., & Woolrich, M. (2014). Fast transient networks in spontaneous human brain activity. *ELife*, *2014*(3). <https://doi.org/10.7554/eLife.01867>
- Becker, M., Sommer, T., & Kühn, S. (2020). Verbal insight revisited: fMRI evidence for early processing in bilateral insulae for solutions with AHA! experience shortly after trial onset. *Human Brain Mapping*, *41*(1), 30–45. <https://doi.org/10.1002/hbm.24785>
- Bertoletti, M., Friel, N., & Rastelli, R. (2015). Choosing the number of clusters in a finite mixture model using an exact integrated completed likelihood criterion. *Metron*, *73*(2), 177–199. <https://doi.org/10.1007/s40300-015-0064-5>
- Biernacki, C., Celeux, G., & Govaert, G. (2000). Assessing a Mixture Model for Clustering with the Integrated Completed Likelihood. *IEEE Transactions on Pattern Analyssi and Machine Intelligence*, *22*(7), 719. [https://doi.org/10.1016/s0965-206x\(98\)80009-0](https://doi.org/10.1016/s0965-206x(98)80009-0)
- Bowden, E., Jung-Beeman, M., Fleck, J., & Kounios, J. (2005). New approaches to demystifying insight. *Trends in Cognitive Sciences*, *9*(7), 322–328. <https://doi.org/10.1016/j.tics.2005.05.012>
- Bowden, E. M., & Jung-Beeman, M. (2003). Aha! Insight experience correlates with solution activation in the right hemisphere. *Psychonomic Bulletin and Review*, *10*(3), 730–737.

- <https://doi.org/10.3758/BF03196539>
- Calhoun, V. D., Liu, J., & Adali, T. (2009). A review of group ICA for fMRI data and ICA for joint inference of imaging, genetic, and ERP data. *NeuroImage*, *45*(1), S163–S172. <https://doi.org/10.1016/J.NEUROIMAGE.2008.10.057>
- Camarda, A., Salvia, É., Vidal, J., Weil, B., Poirel, N., Houdé, O., ... Cassotti, M. (2018). *Neural basis of functional fixedness during creative idea generation: An EEG study*. <https://doi.org/10.1016/j.neuropsychologia.2018.03.009>
- Cao, Z., Li, Y., Hitchman, G., Qiu, J., & Zhang, Q. (2015). Neural correlates underlying insight problem solving: Evidence from EEG alpha oscillations. *Experimental Brain Research*, *233*(9), 2497–2506. <https://doi.org/10.1007/s00221-015-4338-1>
- Cavanagh, J. F., & Shackman, A. J. (2015). Frontal midline theta reflects anxiety and cognitive control: Meta-analytic evidence. *Journal of Physiology Paris*, *109*(1–3), 3–15. <https://doi.org/10.1016/j.jphysparis.2014.04.003>
- Chapeton, J. I., Haque, R., Wittig, J. H., Inati, S. K., & Correspondence, K. A. Z. (2019). Large-Scale Communication in the Human Brain Is Rhythmically Modulated through Alpha Coherence. *Current Biology*, *29*. <https://doi.org/10.1016/j.cub.2019.07.014>
- Cranford, E. A., & Moss, J. (2012). Is Insight Always the Same? A Protocol Analysis of Insight in Compound Remote Associate Problems. *The Journal of Problem Solving*, *4*(2), 128. <https://doi.org/10.7771/1932-6246.1129>
- Delorme, A., & Makeig, S. (2004). EEGLAB: an open source toolbox for analysis of single-trial EEG dynamics including independent component analysis. *Journal of Neuroscience Methods*, *134*(1), 9–21. <https://doi.org/10.1016/J.JNEUMETH.2003.10.009>
- Di Bernardi Luft, C., Zioga, I., Thompson, N. M., Banissy, M. J., & Bhattacharya, J. (2018). Right temporal alpha oscillations as a neural mechanism for inhibiting obvious associations. *Proceedings of the National Academy of Sciences of the United States of America*, *115*(52), E12144–E12152. <https://doi.org/10.1073/pnas.1811465115>
- Doroshenkov, L. G., Konyshov, V. A., & Selishchev, S. V. (2007). Classification of Human Sleep Stages Based on EEG Processing Using Hidden Markov Models. *Biomedical Engineering*, *41*(1), 25–28.
- Erickson, B., Truelove-Hill, M., Oh, Y., Anderson, J., Zhang, F. (Zoe), & Kounios, J. (2018). Resting-state brain oscillations predict trait-like cognitive styles. *Neuropsychologia*, *120*(May), 1–8. <https://doi.org/10.1016/j.neuropsychologia.2018.09.014>
- Fink, A., & Benedek, M. (2014). EEG alpha power and creative ideation. *Neuroscience & Biobehavioral Reviews*, *44*, 111–123. <https://doi.org/10.1016/J.NEUBIOREV.2012.12.002>
- Fink, A., Grabner, R. H., Benedek, M., Reishofer, G., Hauswirth, V., Fally, M., ... Neubauer, A. C. (2009). The creative brain: Investigation of brain activity during creative problem solving by means of EEG and fMRI. *Human Brain Mapping*, *30*(3), 734–748. <https://doi.org/10.1002/hbm.20538>
- Freunberger, R., Klimesch, W., Griesmayr, B., Sauseng, P., & Gruber, W. (2008). Alpha phase coupling reflects object recognition. *NeuroImage*, *42*(2), 928–935. <https://doi.org/10.1016/J.NEUROIMAGE.2008.05.020>
- Gordon, E. M., Laumann, T. O., Gilmore, A. W., Newbold, D. J., Greene, D. J., Berg, J. J., ... Dosenbach, N. U. F. (2017). Precision Functional Mapping of Individual Human Brains. *Neuron*, *95*(4), 791–807.e7. <https://doi.org/10.1016/j.neuron.2017.07.011>
- Grabner, R. H., Fink, A., & Neubauer, A. C. (2007). Brain correlates of self-rated originality of ideas: Evidence from event-related power and phase-locking changes in the EEG.

- Behavioral Neuroscience*, 121(1), 224–230. <https://doi.org/10.1037/0735-7044.121.1.224>
- Janssen, N., Meij, M. van der, López-Pérez, P. J., & Barber, H. A. (2020). Exploring the temporal dynamics of speech production with EEG and group ICA. *Scientific Reports* 2020 10:1, 10(1), 1–14. <https://doi.org/10.1038/s41598-020-60301-1>
- Jung-Beeman, M. (2005). Bilateral brain processes for comprehending natural language. *Trends in Cognitive Sciences*, 9(11), 512–518. <https://doi.org/10.1016/j.tics.2005.09.009>
- Jung-Beeman, M., Bowden, E. M., Haberman, J., Frymiare, J. L., Arambel-Liu, S., Greenblatt, R., ... Kounios, J. (2004). Neural activity when people solve verbal problems with insight. *PLoS Biology*, 2(4), 500–510. <https://doi.org/10.1371/journal.pbio.0020097>
- Kemere, C., Santhanam, G., Yu, B. M., Afshar, A., Ryu, S. I., Meng, T. H., & Shenoy, K. V. (2008). Detecting neural-state transitions using hidden Markov models for motor cortical prostheses. *Journal of Neurophysiology*, 100(4), 2441–2452. <https://doi.org/10.1152/jn.00924.2007>
- Klimesch, W., Doppelmayr, M., Pachinger, T., & Russegger, H. (1997). Event-related desynchronization in the alpha band and the processing of semantic information. *Brain Research. Cognitive Brain Research*, 6(2), 83–94. [https://doi.org/10.1016/S0926-6410\(97\)00018-9](https://doi.org/10.1016/S0926-6410(97)00018-9)
- Klimesch, W., Fellinger, R., & Freunberger, R. (2011). Alpha oscillations and early stages of visual encoding. *Frontiers in Psychology*, 2(MAY), 1–11. <https://doi.org/10.3389/fpsyg.2011.00118>
- Klimesch, W., Doppelmayr, M., Schwaiger, J., Auinger, P., & Winkler, T. (1999). “Paradoxical” alpha synchronization in a memory task. In *Cognitive Brain Research* (Vol. 7).
- Klimesch, Wolfgang. (2012). Alpha-band oscillations, attention, and controlled access to stored information. *Trends in Cognitive Sciences*, 16(12), 606–617. <https://doi.org/10.1016/j.tics.2012.10.007>
- Kounios, J., Frymiare, J. L., Bowden, E. M., Fleck, J. I., Subramaniam, K., Parrish, T. B., & Jung-Beeman, M. (2006). The Prepared Mind Neural Activity Prior to Problem Presentation Predicts Subsequent Solution by Sudden Insight. *Psychological Science*, 17(10), 882–890.
- Kounios, John, & Beeman, M. (2014). The Cognitive Neuroscience of Insight. *Annual Review of Psychology*, 65, 71–93. <https://doi.org/10.1146/annurev-psych-010213-115154>
- Kounios, John, Fleck, J. I., Green, D. L., Payne, L., Stevenson, J. L., Bowden, E. M., & Jung-Beeman, M. (2008). The origins of insight in resting-state brain activity. *Neuropsychologia*, 46(1), 281–291. <https://doi.org/10.1016/J.NEUROPSYCHOLOGIA.2007.07.013>
- Laukkonen, R. E., Schooler, J. W., Tangen, J. M., & Laukkonen, R. (2018). *The Eureka Heuristic: Relying on insight to appraise the quality of ideas*.
- Lederman, D., & Tabrikian, J. (2012). Classification of multichannel EEG patterns using parallel hidden Markov models. *Med Biol Eng Comput*, 50, 319–328. <https://doi.org/10.1007/s11517-012-0871-2>
- Lundqvist, M., Rose, J., Herman, P., Brincat, S. L., Buschman, T. J., Miller, E. K., ... Miller, E. K. (2016). Gamma and Beta Bursts Underlie Working Memory Article Gamma and Beta Bursts Underlie Working Memory. *Neuron*, 90(1), 152–164. <https://doi.org/10.1016/j.neuron.2016.02.028>
- Makeig, S., Debener, S., Onton, J., & Delorme, A. (2004). Mining event-related brain dynamics. *Opinion TRENDS in Cognitive Sciences*, 8(5). <https://doi.org/10.1016/j.tics.2004.03.008>
- Martindale, C., & Mines, D. (1975). Creativity and cortical activation during creative, intellectual and eeg feedback tasks. *Biological Psychology*, 3(2), 91–100.

- [https://doi.org/10.1016/0301-0511\(75\)90011-3](https://doi.org/10.1016/0301-0511(75)90011-3)
- Neuper, C., Pfurtscheller, G., Obermaier, B., Guger, C., Neuper, C., & Pfurtscheller, G. (2001). Hidden Markov models for online classification of single trial EEG data. *Pattern Recognition Letters*, 22, 1299–1309. [https://doi.org/10.1016/S0167-8655\(01\)00075-7](https://doi.org/10.1016/S0167-8655(01)00075-7)
- Nunez, P. L., Silberstein, R. B., Cadusch, P. J., Wijesinghe, R. S., Westdorp, A. F., & Srinivasan, R. (1994). A theoretical and experimental study of high resolution EEG based on surface Laplacians and cortical imaging. *Electroencephalography and Clinical Neurophysiology*, 90(1), 40–57. [https://doi.org/10.1016/0013-4694\(94\)90112-0](https://doi.org/10.1016/0013-4694(94)90112-0)
- Oh, Y., Chesebrough, C., Erickson, B., Zhang, F., & Kounios, J. (2020). An insight-related neural reward signal. *NeuroImage*, 214, 116757. <https://doi.org/10.1016/j.neuroimage.2020.116757>
- Onton, J., Westerfield, M., Townsend, J., & Makeig, S. (2006). Imaging human EEG dynamics using independent component analysis. *Neuroscience & Biobehavioral Reviews*, 30(6), 808–822. <https://doi.org/10.1016/J.NEUBIOREV.2006.06.007>
- Quinn, A. J., Vidaurre, D., Abeysuriya, R., Becker, R., Nobre, A. C., & Woolrich, M. W. (2018). Task-Evoked Dynamic Network Analysis Through Hidden Markov Modeling. *Frontiers in Neuroscience*, 12(AUG), 603. <https://doi.org/10.3389/fnins.2018.00603>
- Rabiner, L. R., & Juang, B. H. (1986). An Introduction to Hidden Markov Models. *IEEE ASSP Magazine*, 3(1), 4–16. <https://doi.org/10.1109/MASSP.1986.1165342>
- Rominger, C., Papousek, I., Perchtold, C. M., Benedek, M., Weiss, E. M., Weber, B., ... Fink, A. (2020). Functional coupling of brain networks during creative idea generation and elaboration in the figural domain. *NeuroImage*, 207, 116395. <https://doi.org/10.1016/J.NEUROIMAGE.2019.116395>
- Rothmaler, K., Nigbur, R., & Ivanova, G. (2017). New insights into insight: Neurophysiological correlates of the difference between the intrinsic “aha” and the extrinsic “oh yes” moment. *Neuropsychologia*, 95, 204–214. <https://doi.org/10.1016/j.neuropsychologia.2016.12.017>
- Rukat, T., Baker, A., Quinn, A., & Woolrich, M. (2016). *Resting state brain networks from EEG: Hidden Markov states vs. classical microstates*. Retrieved from <http://arxiv.org/abs/1606.02344>
- Salvi, C., Bricolo, E., Franconeri, S. L., Kounios, J., & Beeman, M. (2015). Sudden insight is associated with shutting out visual inputs. *Psychonomic Bulletin and Review*, 22(6), 1814–1819. <https://doi.org/10.3758/s13423-015-0845-0>
- Salvi, C., Simoncini, C., Grafman, J., & Beeman, M. (2020). Oculometric signature of switch into awareness? Pupil size predicts sudden insight whereas microsaccades predict problem-solving via analysis. *NeuroImage*, 217, 116933. <https://doi.org/10.1016/j.neuroimage.2020.116933>
- Samaha, J., Iemi, L., Haegens, S., & Busch, N. A. (2020). Spontaneous Brain Oscillations and Perceptual Decision-Making. *Trends in Cognitive Sciences*, 1–15. <https://doi.org/10.1016/j.tics.2020.05.004>
- Santaracchi, E., Sprugnoli, G., Bricolo, E., Costantini, G., Liew, S. L., Musaeus, C. S., ... Rossi, S. (2019). Gamma tACS over the temporal lobe increases the occurrence of Eureka! moments. *Scientific Reports*, 9(1), 1–12. <https://doi.org/10.1038/s41598-019-42192-z>
- Schooler, J. W., & Melcher, J. (1995). The ineffability of insight. *The Creative Cognition Approach*, 97–133.
- Schwab, D., Benedek, M., Papousek, I., Weiss, E. M., & Fink, A. (2014). The time-course of EEG alpha power changes in creative ideation. *Frontiers in Human Neuroscience*, 8(MAY).

- <https://doi.org/10.3389/fnhum.2014.00310>
- Seedat, Z. A., Quinn, A. J., Vidaurre, D., Liuzzi, L., Gascoyne, L. E., Hunt, B. A. E., ... Brookes, M. J. (2020). The role of transient spectral ‘bursts’ in functional connectivity: A magnetoencephalography study. *NeuroImage*, *209*, 116537. <https://doi.org/10.1016/j.neuroimage.2020.116537>
- Shappell, H. M., Duffy, K. A., Rosch, K. S., Pekar, J. J., Mostofsky, S. H., Lindquist, M. A., & Cohen, J. R. (2021). Children with attention-deficit/hyperactivity disorder spend more time in hyperconnected network states and less time in segregated network states as revealed by dynamic connectivity analysis. *NeuroImage*, *229*, 117753. <https://doi.org/10.1016/j.neuroimage.2021.117753>
- Sprugnoli, G., Rossi, S., Emmendorfer, A., Rossi, A., Liew, S. L., Tatti, E., ... Santarnecchi, E. (2017). Neural correlates of Eureka moment. *Intelligence*, *62*(March), 99–118. <https://doi.org/10.1016/j.intell.2017.03.004>
- Sternberg, R. J., Davidson, J. E., & Simonton, D. K. (1995). Foresight in Insight? A Darwinian Answer. In *The Nature of Insight*. <https://doi.org/10.1521/00332747.1941.11022320>
- Stevner, A. B. A., Vidaurre, D., Cabral, J., Rapuano, K., Nielsen, S. F. V., Tagliazucchi, E., ... Kringsbach, & M. L. (2019). Discovery of key whole-brain transitions and dynamics during human wakefulness and non-REM sleep. *Nature Communications*. <https://doi.org/10.1038/s41467-019-08934-3>
- Subramaniam, K., Kounios, J., Parrish, T. B., & Jung-Beeman, M. (2008). A Brain Mechanism for Facilitation of Insight by Positive Affect. *Journal of Cognitive Neuroscience*, *21*(3), 4115–4432.
- Tenke, C. E., & Kayser, J. (2012). Generator localization by current source density (CSD): Implications of volume conduction and field closure at intracranial and scalp resolutions. *Clinical Neurophysiology*, *123*(12), 2328–2345. <https://doi.org/10.1016/J.CLINPH.2012.06.005>
- Vidaurre, D., Hunt, L. T., Quinn, A. J., Hunt, B. A. E., Brookes, M. J., Nobre, A. C., & Woolrich, M. W. (2018). Spontaneous cortical activity transiently organises into frequency specific phase-coupling networks. *Nature Communications*, *9*(1), 1–13. <https://doi.org/10.1038/s41467-018-05316-z>
- Vrieze, S. I. (2012). Model selection and psychological theory: A discussion of the differences between the Akaike information criterion (AIC) and the Bayesian information criterion (BIC). *Psychological Methods*, *17*(2), 228–243. <https://doi.org/10.1037/a0027127>
- Webb, M. E., Little, D. R., & Cropper, S. J. (2016). Insight Is Not in the Problem: Investigating Insight in Problem Solving across Task Types. *Frontiers in Psychology*, *7*(SEP), 1424. <https://doi.org/10.3389/fpsyg.2016.01424>
- Williams, N. J., Daly, I., & Nasuto, S. J. (2018). Markov Model-Based Method to Analyse Time-Varying Networks in EEG Task-Related Data. *Frontiers in Computational Neuroscience*, *12*, 76. <https://doi.org/10.3389/fncom.2018.00076>
- Zhou, S., Chen, S., Wang, S., Zhao, Q., Zhou, Z., & Lu, C. (2018). Temporal and Spatial Patterns of Neural Activity Associated with Information Selection in Open-ended Creativity. *Neuroscience*, *371*, 268–276. <https://doi.org/10.1016/J.NEUROSCIENCE.2017.12.006>

Tables

Table 1. State probabilities immediately before onset

Mean and Standard Errors are shown for each hidden state

Peak Activation	S1 Alpha	S2 Gamma	S3 Theta	S4 Theta	S5 Theta	S6 Theta	S3 Theta
Mean	0.123	0.136	0.293	0.137	0.126	0.094	0.091
SE	(0.004)	(0.004)	(0.006)	(0.004)	(0.004)	(0.003)	(0.004)

Table 2: Characteristics of the last alpha-state before response.

For each decoded trial, the last alpha-state before response was identified. We computed the number of transitions (between all other states) and total time from the end of that state to the response; we also computed the duration of the last alpha-state. Mean and standard errors for each case were shown.

	# transitions to response	ms to response	Duration
ANA	8.32(0.24)	3905.11(97.68)	600.32(19.69)
INS	7.19(0.18)	3532.45(79.07)	687.12(18.35)

Figures

Figure 1. Hidden Markov Model

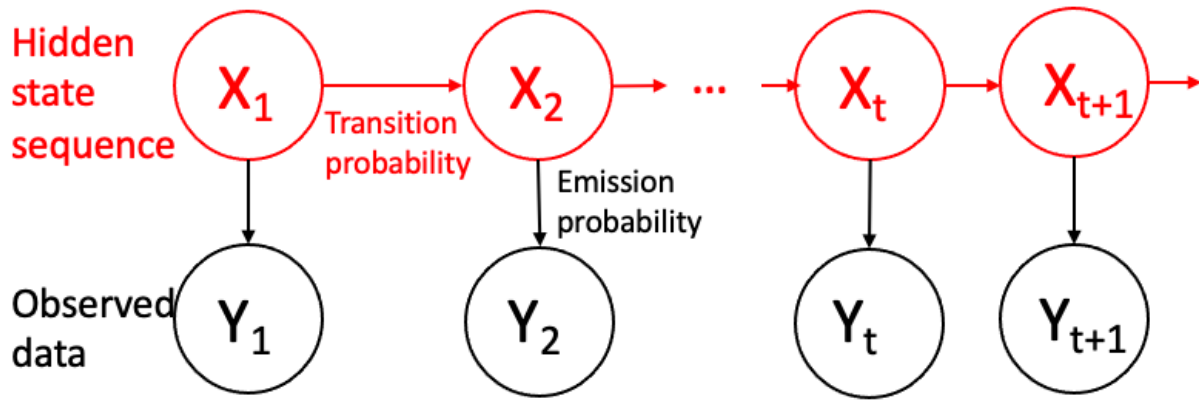


Figure 1 An illustration of the hidden Markov model

Figure 2.

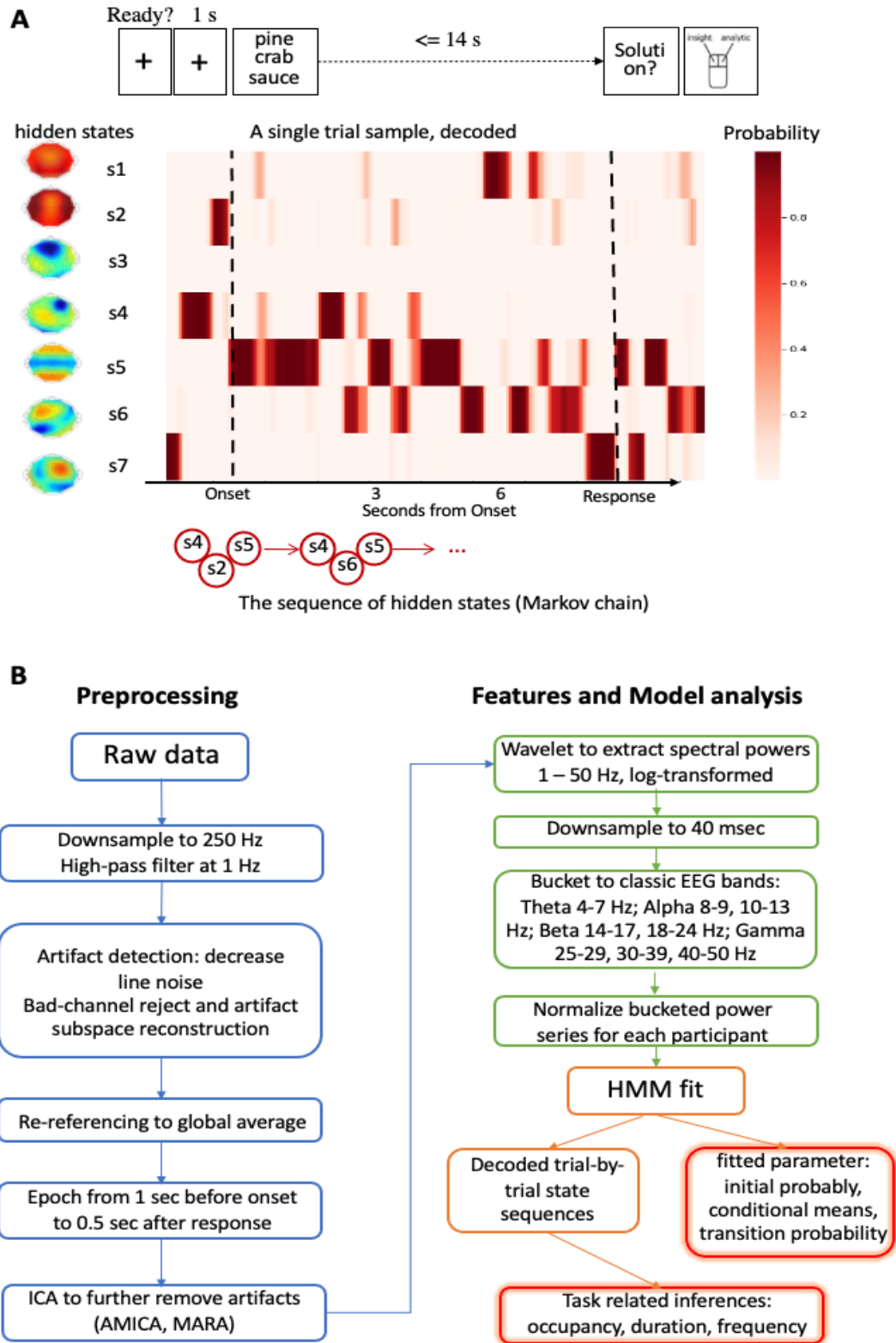


Figure 2. The experiment and processing paradigm.

A: Experiment procedure and a sample decoded trial. Probabilities of hidden states, s_1, \dots, s_7 , are indicated by the color shade, as a function of time (onset-locked); Thumbnail topographies indicate the activation patterns of the hidden states in its most active frequency band; The resulting Markov chain decoded from the trial is shown at the bottom.

B: Analysis steps including preprocessing (blue), feature construction (green), model fitting and inferences (orange)

Figure 3. Model Order Comparison

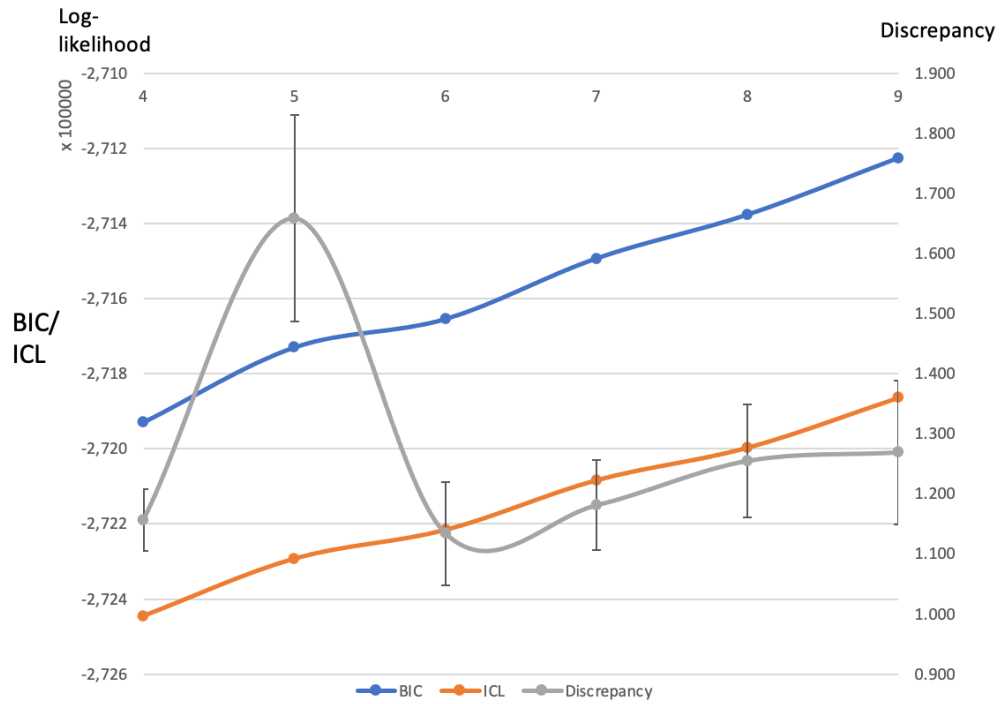


Figure 3. Model Fitting

Three model fitting measures are plotted against the number of hidden states. BIC: Bayesian Information Criterion; ICL: Integrated Complete Likelihood; Discrepancy: Average differences between two fitted models over split-half data. 8 iterations were run for each state number. Larger difference is associated with lower stability.

Figure 4. Hidden states

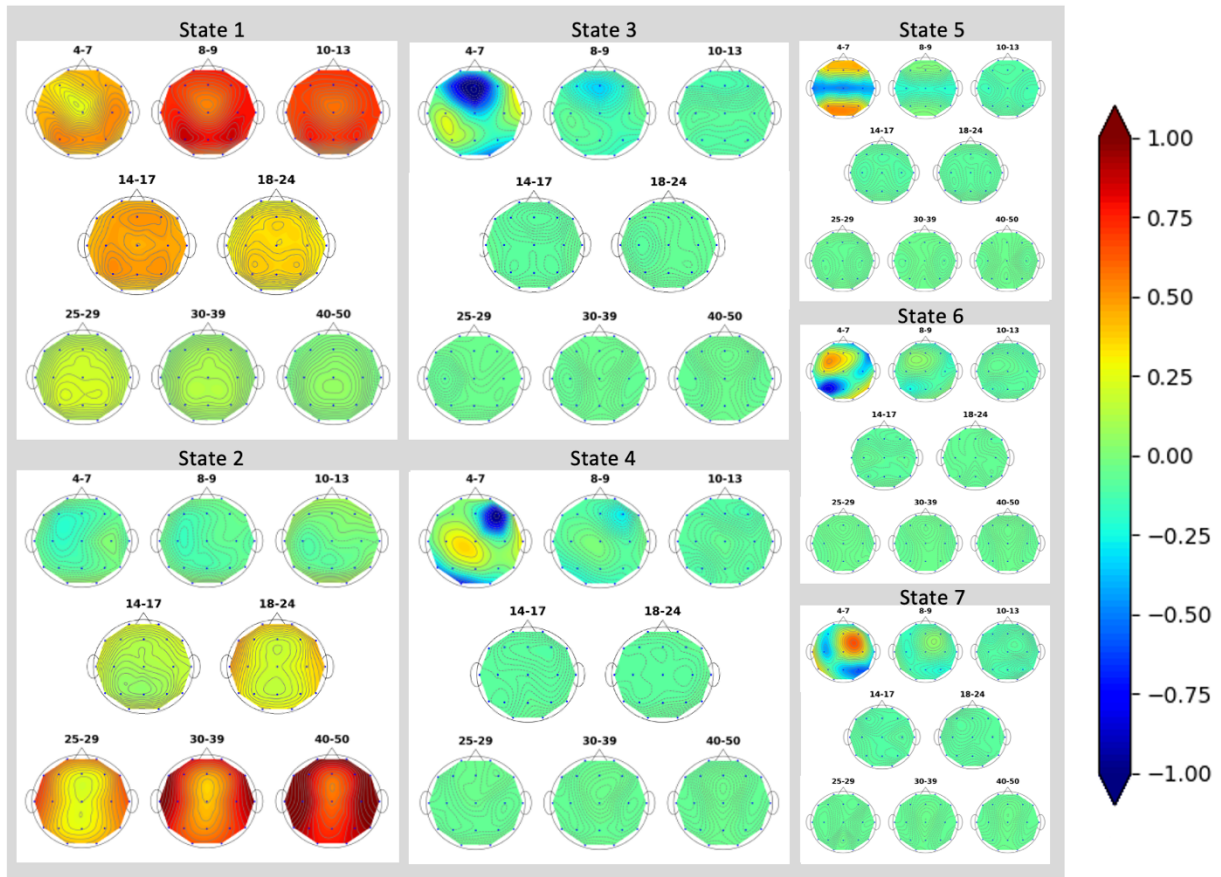


Figure 4. Hidden states

Seven hidden states identified by HMM, characterized by the mean power topography in classic EEG frequency bands: Theta band (4-7 Hz), low and high Alpha bands (8-9 Hz and 10-13 Hz), low and high Beta bands (14-17 Hz, 18-24 Hz), and three Gamma bands (25-29 Hz, 30-39 Hz, 40-50 Hz).

Figure 5. Dynamic characteristics of hidden states

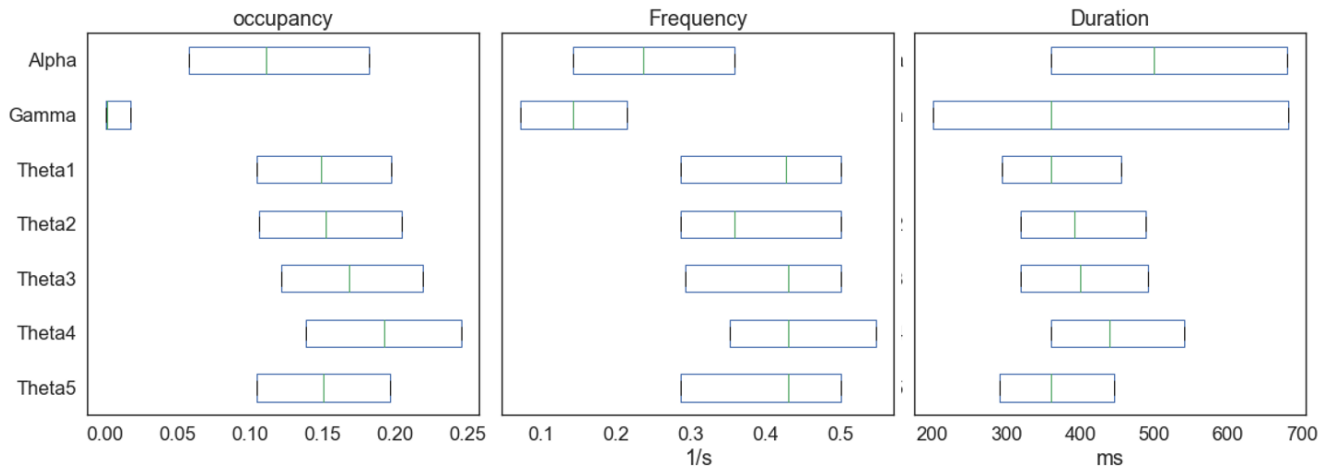


Figure 5. Dynamic characteristics of hidden states. Mean and 25%-75% quantile of each metrics are shown.

Left: Occupancy (average probability during the trial) of each hidden state; middle: Frequency or the number of visits per second; right: visit duration.

Figure 6. Alpha-state probability

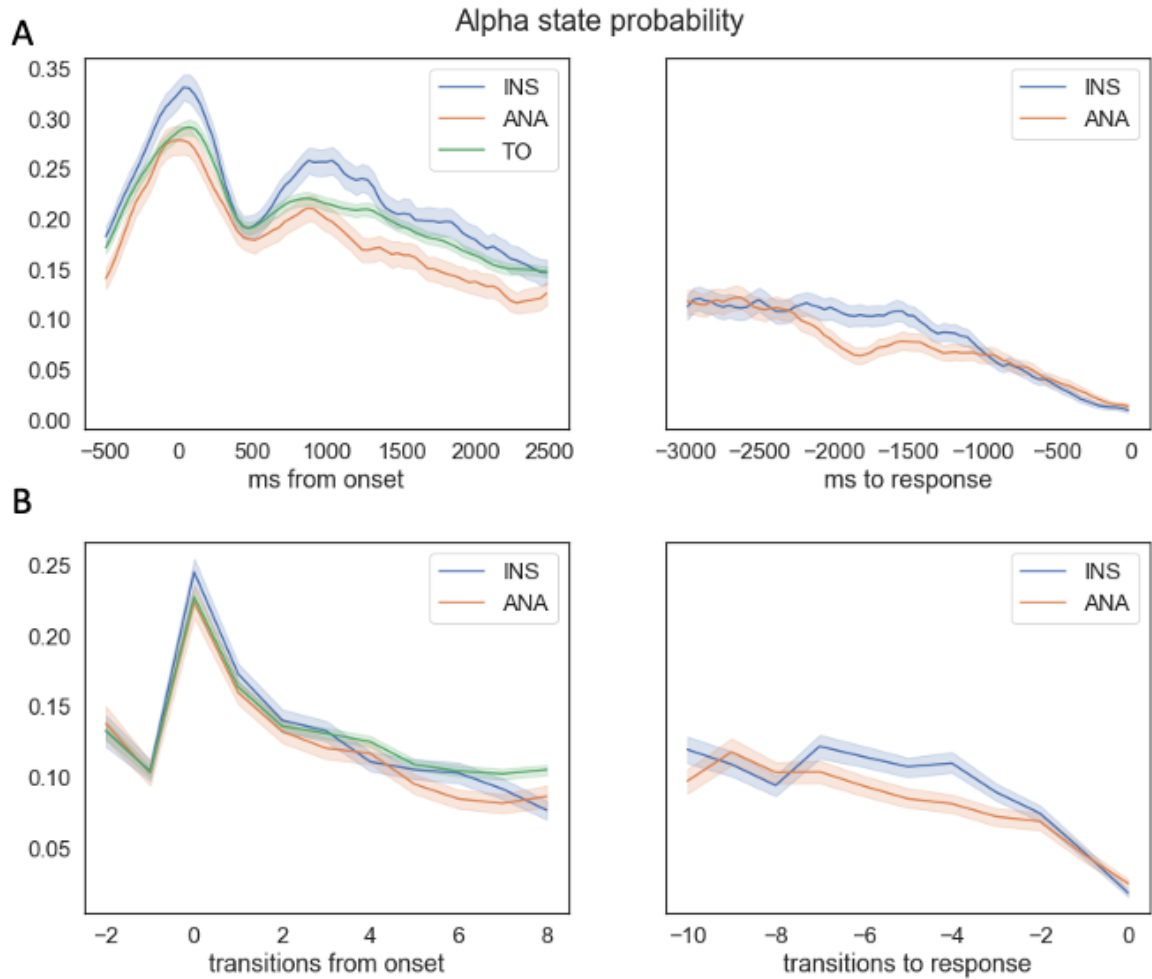


Figure 6. Time course of the alpha-state probability

A: trials aligned by milliseconds. Left: onset-locked. To minimize the onset-response interaction, data points within 2 seconds to response were excluded. Right: response-locked. Data points within the first 2 seconds from onset were excluded.

B: trials aligned by number of state transitions: Left: onset-locked; right: response-locked.

Colored band shows 1-se range around the mean. 0 marks are aligned between the top and bottom rows, but the x-axis units do not align. Corresponding results for other hidden states are included in Supplement 2.

Figure 7. Alpha-state characteristic by stages

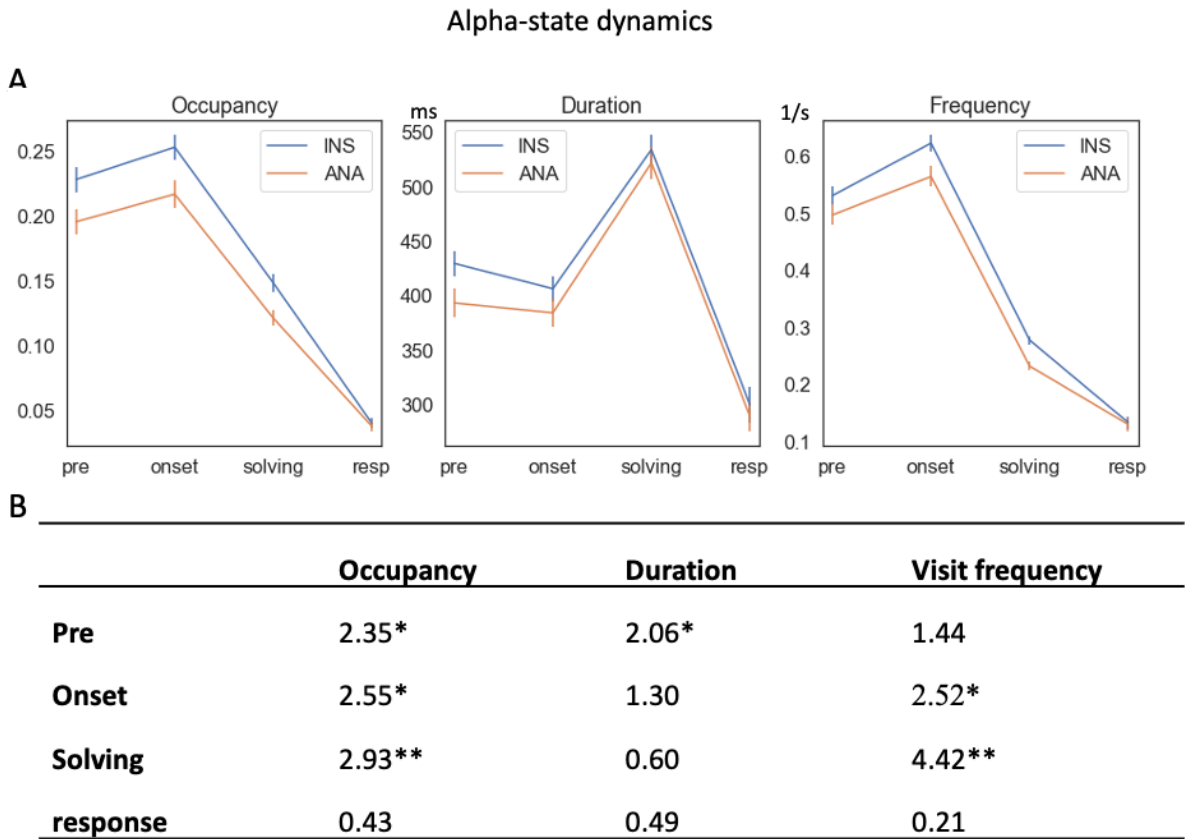


Figure 7. Alpha-state dynamics

A: trials were temporally bucketed into four stages: pre-stage (1-second interval immediately before onset), onset stage (1-second interval immediately following onset), response stage (1-second interval before response) and solving stage (the trial period in between the onset and response stage). Graphs show the alpha-state occupancy, duration per visit and visit frequency for trials solved with insight, trials solved with analysis and time-out trials.

B: z-score for INS trials – ANA trials in each of the four stages.

*p-value<0.05; **p-value<0.01, two-tailed

Corresponding results for other hidden states are shown in Supplement 4.

Figure 8. Duration of states

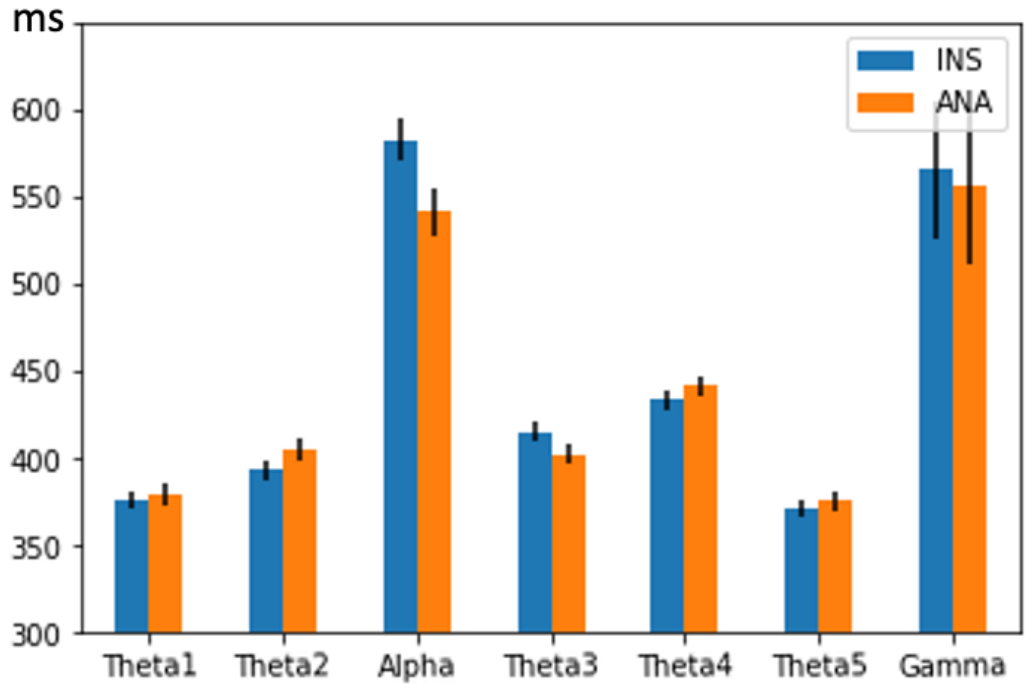


Figure 8. Duration per visit for each hidden state

Figure 9. Alpha-state probability changes before response: INS - ANA

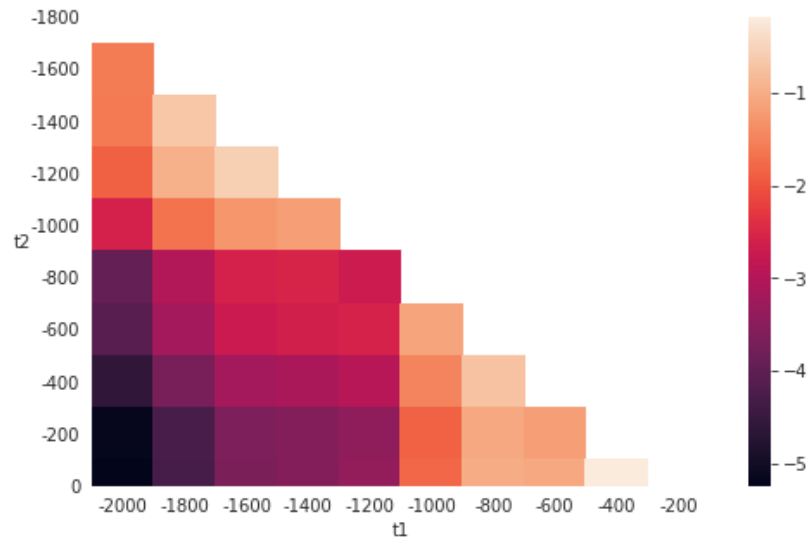
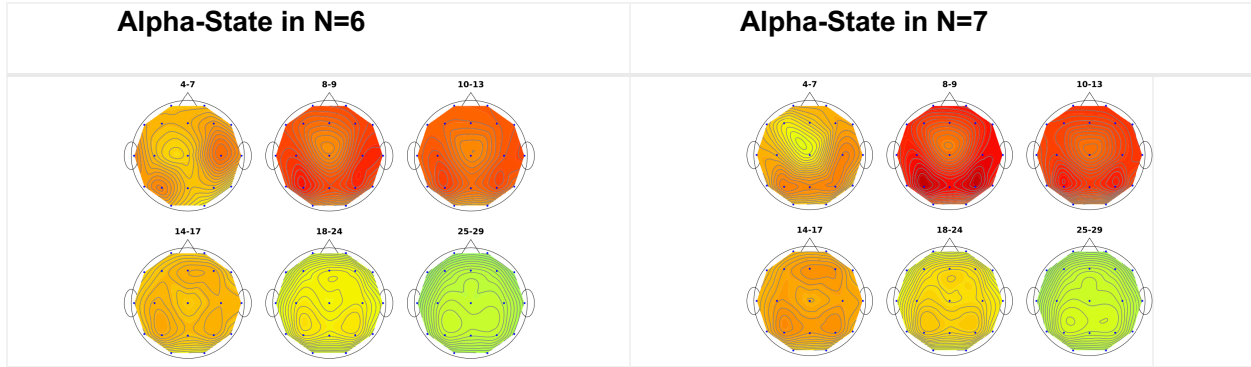


Figure 9 Alpha-state probability changes before response: INS - ANA

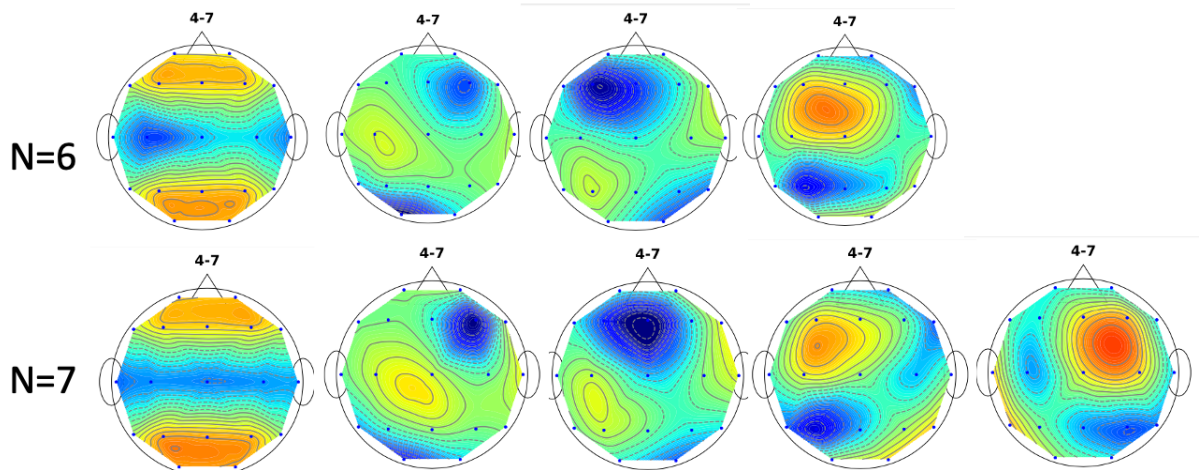
Trials solved with insight were associated with a steeper decline of alpha-state probability compared to trials solved with analysis. Heatmap shows the z-score (INS-ANA) of the changes during different sliding windows prior to response, from t_1 to t_2 . E.g., the lower-left corner represents the difference in the change from 2 seconds ($t_1 = -2000$) before response to the moment of response ($t_2 = 0$).

Supplements

Supplement 1. Comparison of model fit with N=6 and N=7

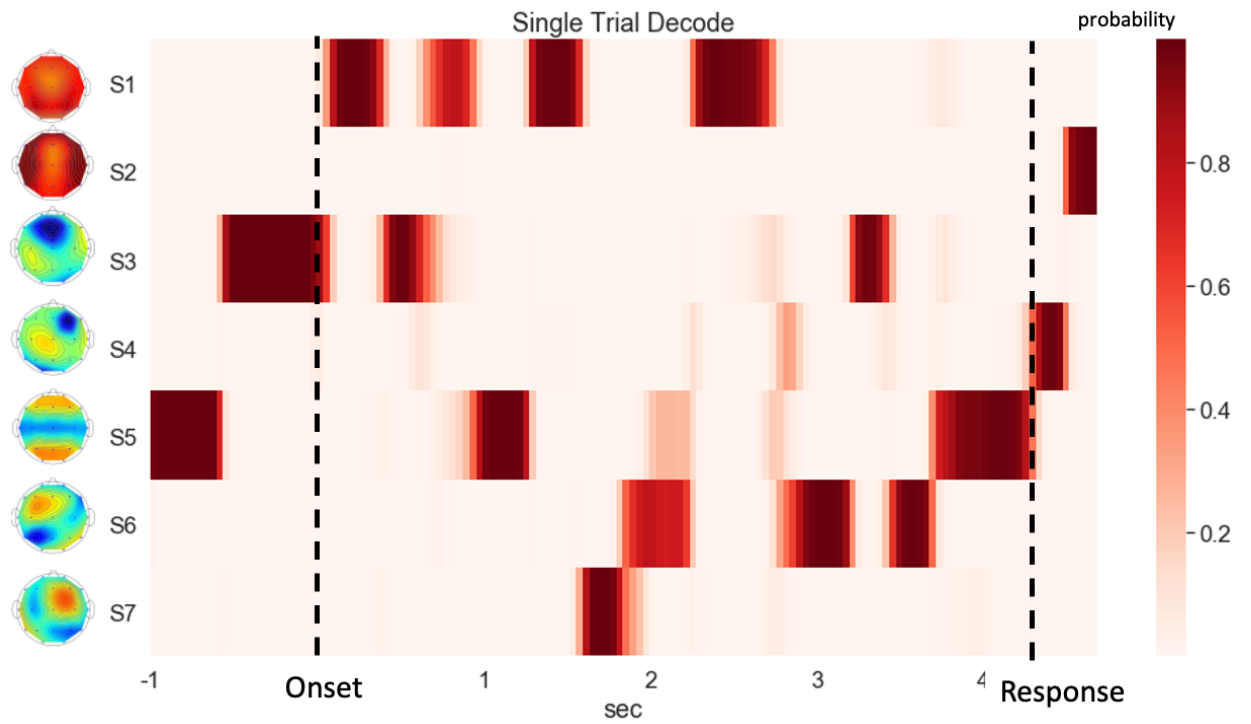


Theta States



HMM with N=6 and N=7 yielded similar results. The alpha-state and gamma state (not shown) are almost identical. One of the theta states in N=6 split into two the state in N=7.

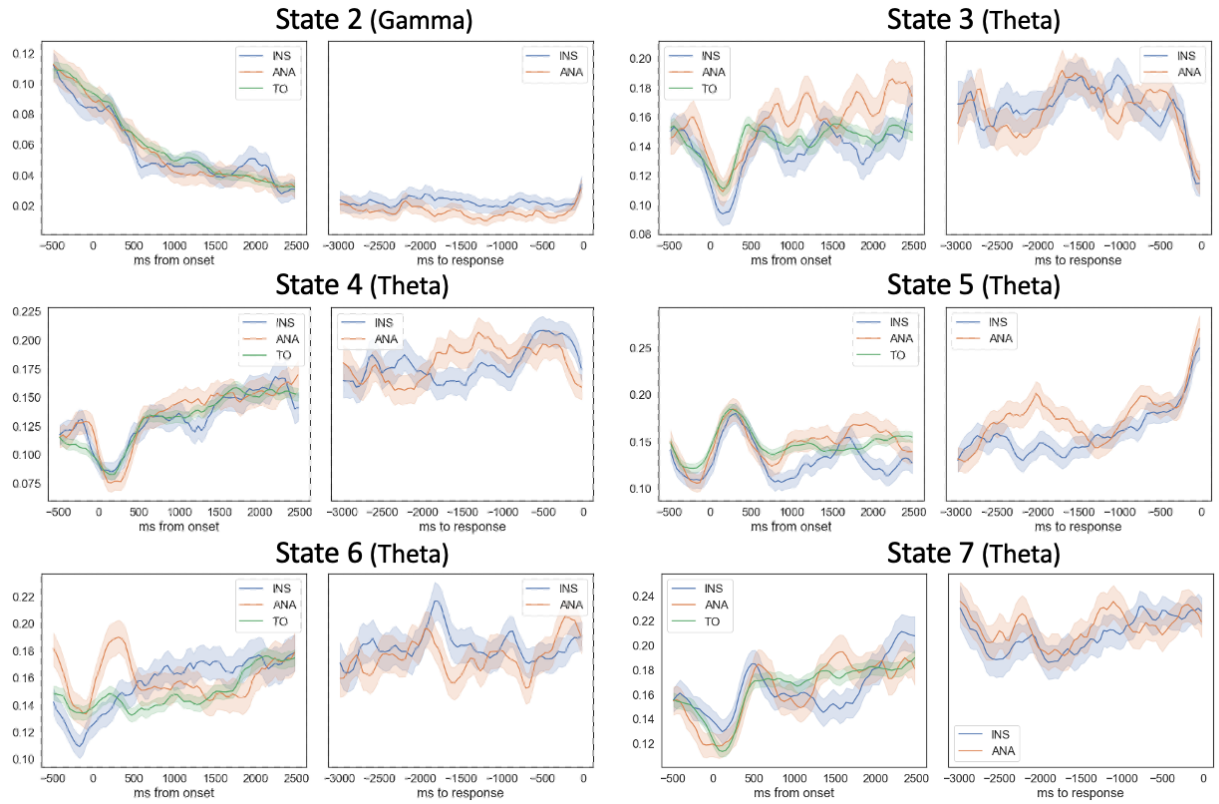
Supplement 2. A sample of decoded trial



An example of solved trials is shown above, with model inferred state probabilities. Participant indicated “solved with analysis” for this trial.

Supplement 3. Time course of state probabilities

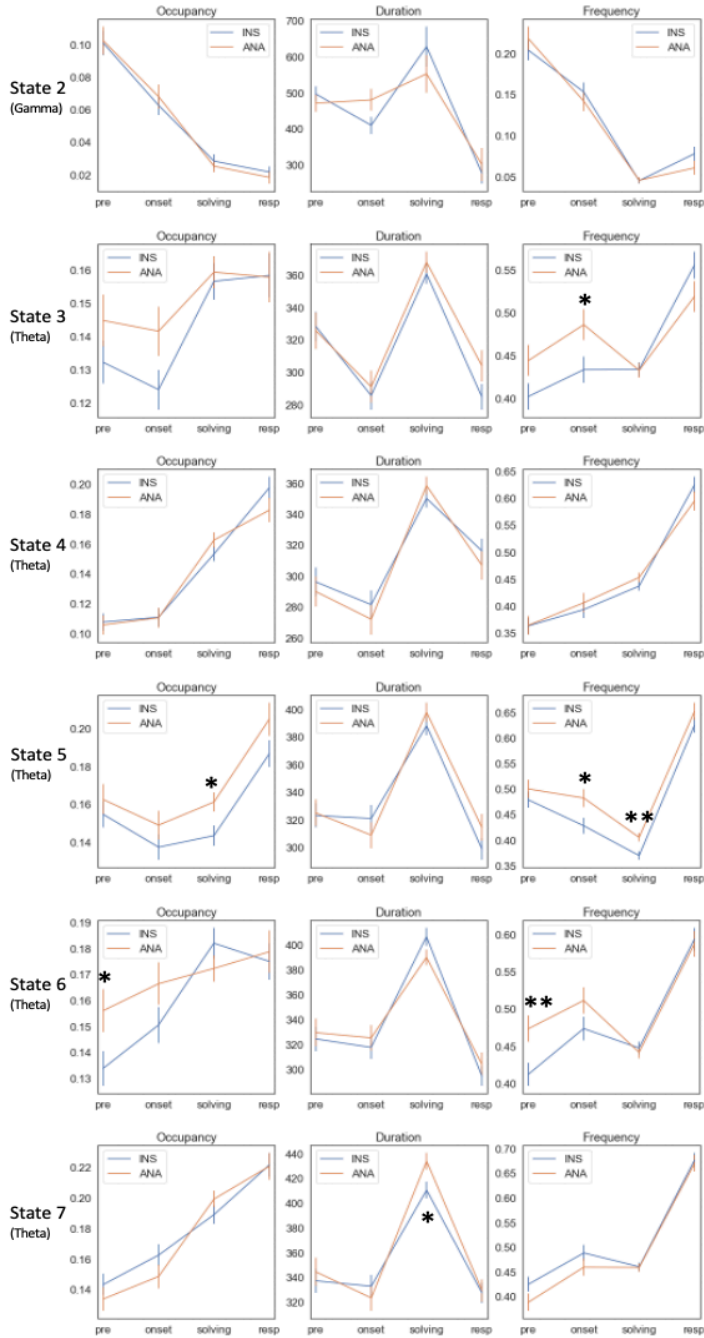
Similar to Fig. 6A, the time course for states 2 – 7 are shown below



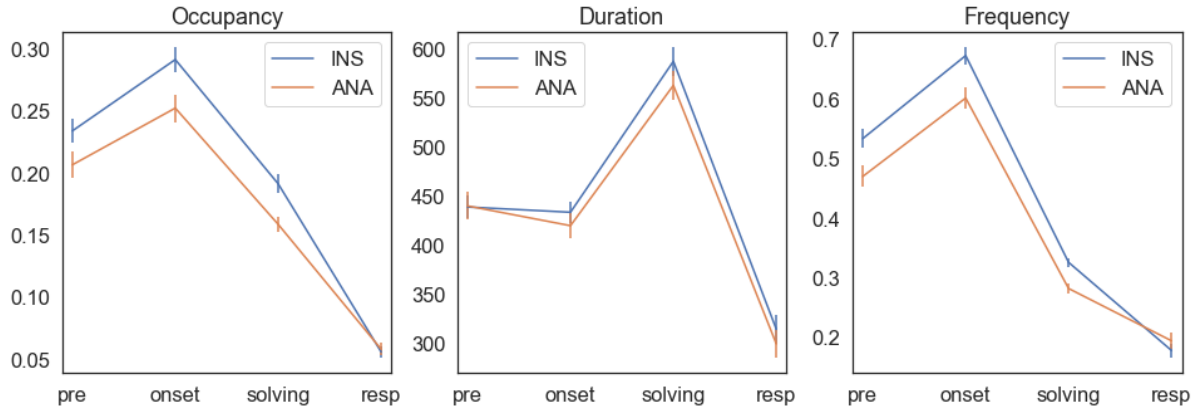
State 1 is the alpha-state, which is provided in the main text.

Supplement 4. four-stage analysis comparing INS versus ANA

Similar to Fig. 7, occupancy, duration (ms) and frequencies (1/s) bucketed by solving stage are provided below for each hidden states 2 – 7. *, ** indicate p-value < 0.05 and < 0.01, two-tailed, respectively.



Supplement 5. 4-stage analyses of alpha-state and trial outcomes interaction when fitting models with different numbers of states
N=6

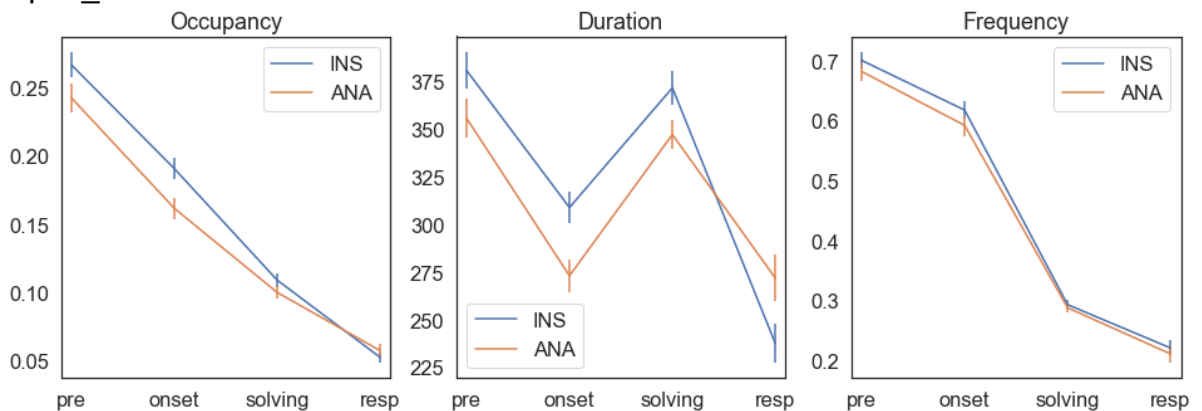


	Occupancy	Duration	Visit frequency
N=6			
Pre	1.91	-0.06	2.68**
Onset	2.58**	0.81	3.14*
Solving	3.27**	1.18	4.03**
response	-0.32	0.74	-0.89

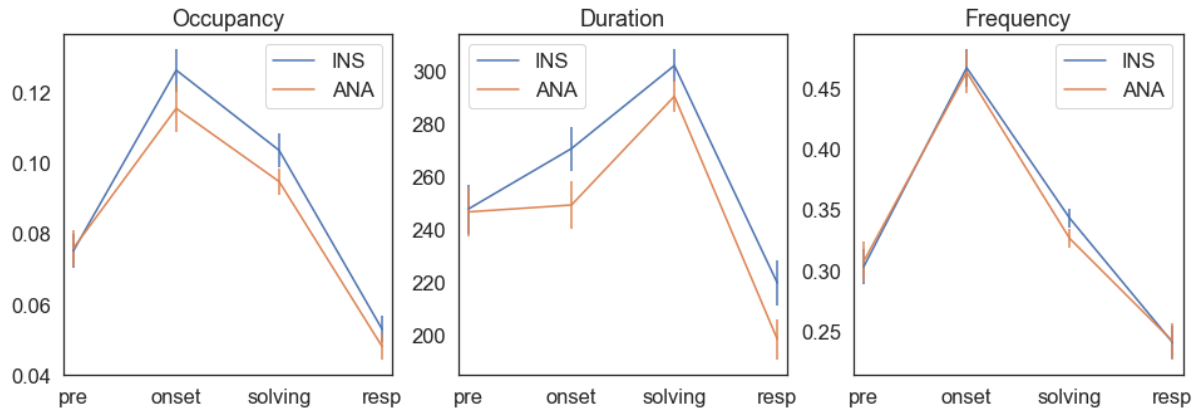
N=8

With 8 states, the model identified two states featuring alpha band activation. One peaks at the lower alpha band in the frontal and occipital regions; the other peaks at the upper alpha band with bilateral parietal activation. Data from both alpha-states are presented here.

Alpha_lower



Alpha_upper



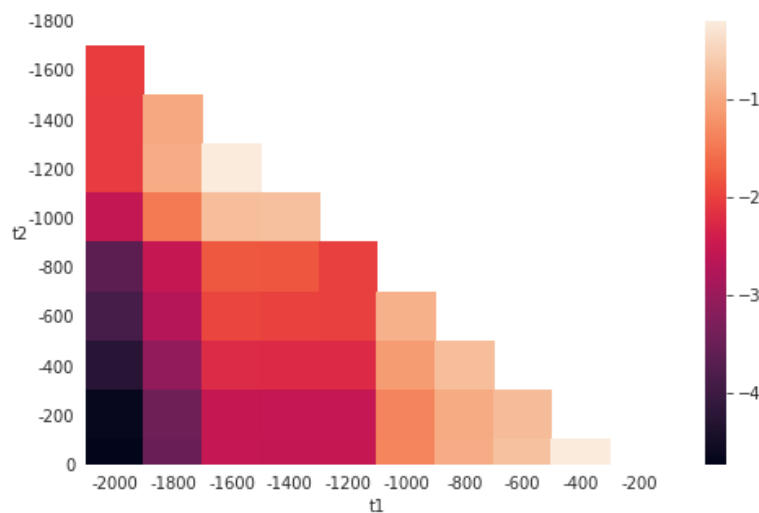
Alpha_lower	Occupancy	Duration	Visit frequency
Pre	1.73	1.72	0.85
Onset	2.63**	2.91**	1.10
Solving	1.27	2.16*	0.49
response	-0.78	-2.20*	0.51

Alpha_upper	Occupancy	Duration	Visit frequency
Pre	-0.04	0.21	-0.17
Onset	1.25	1.63	0.23
Solving	1.53	1.32	1.30
response	0.87	1.88	-0.15

Supplement 6. Alpha-state probability changes before response: INS vs ANA

To control for the different distributions of RT of solving with insight and solving with analysis, we repeated the analysis in Fig. 9 with a subset of trials. We randomly excluded 10% of analysis trials whose RT was above 85% quantile, and 10% of insight trials whose RT was below 15% quantile. This results in similar average RT: 6190 ± 92 msec insight trials and 6091 ± 97 msec for analysis trials.

The result is similar to Fig. 9, indicating that the steeper decline of alpha-state on insight trials, relative to analysis trials, is not due to the difference in RT.



Alpha-state probability changes before response: INS - ANA

Trials solved with insight were associated with a steeper decline of alpha-state probability compared to trials solved with analysis. Heatmap shows the z-score (INS-ANA) of the changes during different sliding windows prior to response, from t_1 to t_2 . E.g., the lower-left corner represents the difference in the change from 2 seconds ($t_1 = -2000$) before response to the moment of response ($t_2 = 0$).